Received: 5 January 2024 | Revised: 23 April 2024 | Accepted: 31 May 2024

DOI: 10.1111/mec.17437

ORIGINAL ARTICLE

MOLECULAR ECOLOGY WILEY

Ecological transcriptomics reveals stress response pathways of a ground-herb species in a waterlogging gradient of Amazonian riparian forests

Clarisse Palma-Silva[1] | Amanda F. Mortati[2] | Cleber Juliano Neves Chaves[1] | Bárbara Simões Santos Leal[1,3] | Rafael V. Ribeiro[4] | Fabio Pinheiro[1] | Milene Ferro[5] | Diego M. Riaño-Pachón[6] | Jacqueline Salvi de Mattos[1] | Marília Manupella Tavares[1] | Paulo Aecyo[1] | Tami da Costa Cacossi[1] | Jochen Schöngart[7] | Maria Teresa Fernandez Piedade[7] | Thiago André[2,8]

[1]Laboratory of Evolutionary Ecology and Genomics of Neotropical Plants, Department of Plant Biology, Institute of Biology, Universidade Estadual de Campinas, Campinas, São Paulo, Brazil

[2]Institute of Biodiversity and Forests, Universidade Federal do Oeste do Pará, Santarém, Pará, Brazil

[3]Vale Institute of Technology Sustainable Development, Belém, Pará, Brazil

[4]Laboratory of Crop Physiology—Department of Plant Biology, Institute of Biology, Universidade Estadual de Campinas, Campinas, São Paulo, Brazil

[5]São Paulo State University (UNESP), Institute of Biosciences, Rio Claro, São Paulo, Brazil

[6]Laboratory of Computational, Evolutionary, and Systems Biology, Centro de Energia Nuclear na Agricultura, Universidade de São Paulo, Piracicaba, São Paulo, Brazil

[7]Ecology, Monitoring and Sustainable Use of Wetlands (MAUA Research Group), National Institute for Amazon Research (INPA), Manaus, Amazonas, Brazil

[8]Botany Department, Institute of Biological Sciences; Universidade de Brasília, Brasília, Distrito Federal, Brazil

Correspondence
Clarisse Palma-Silva and Bárbara Simões Santos Leal, Laboratory of Evolutionary Ecology and Genomics of Neotropical Plants – Department of Plant Biology, Institute of Biology, Universidade Estadual de Campinas, Campinas, São Paulo, Brazil.
Email: clarissepalma@yahoo.com.br and bssleal@gmail.com

Funding information
Fundação Amazônia Paraense de Amparo à Pesquisa, Grant/Award Number: 067/2020; Conselho Nacional de Desenvolvimento Científico e Tecnológico, Grant/Award Number: 302962/2022-0, 304295/2022-1, 311558/2021-6 and 302849/2021-1; Fundação de Amparo à Pesquisa do Estado de São Paulo, Grant/Award Number: 2019/24823-2 and 2021/10639-5

Handling Editor: Samridhi Chaturvedi

Abstract

Environmental stress is a fundamental facet of life and a significant driver of natural selection in the wild. Gene expression diversity may facilitate adaptation to environmental changes, without necessary genetic change, but its role in adaptive divergence remains largely understudied in Neotropical systems. In Amazonian riparian forests, species distribution is predominantly influenced by species' waterlogging tolerance. The flooding gradient delineates distinct wetland forest types, shaping habitats and species characteristics. Here we investigated the molecular basis of environmental stress response in a tropical ground-herb species (*Ischnosiphon puberulus*) to environmental variation in Amazonian riparian forests. We compared environmental variables and gene expression profiles from individuals collected in two forest types: *Igapó* and *Terra firme* in the Amazonian riparian forests. Predictable seasonal flooding poses a significant challenge in *Igapó* compared to *Terra firme* environments, with the former presenting higher water column height and longer flooding duration. Our findings suggest that contrasting environmental conditions related to flooding regimes are important drivers of population genetic differentiation and differential gene expression in *I. puberulus*. Enriched gene ontology terms highlight associations with environmental stresses, such as defence response, water transport, phosphorylation, root development, response

to auxin, salicylic acid and oxidative stress. By uncovering key environmental stress response pathways conserved across populations, *I. puberulus* offers novel genetic insights into the molecular basis of plant reactions to environmental constraints found in flooded areas of this highly biodiverse neotropical ecosystem.

KEYWORDS
adaptation, Amazonian forest, differential gene expression, Neotropical biomes, population genetics – empirical

1 | INTRODUCTION

Environmental stress constitutes a fundamental aspect of life and a significant driver of natural selection in the wild. The study of environmental stress responses at the genomic level has provided important insights into the mechanisms underpinning the ability of species to thrive in environmental gradients (Van Straalen & Roelofs, 2011). However, most research on genome and transcriptomic environmental stress analyses focus on model organisms subjected to stress factors within experimental and control conditions (Penna & Naithani, 2022). Nevertheless, there remains a notable gap in research concerning organisms surviving, growing and reproducing under natural conditions, particularly within complex gradients of environmental stress. Population heterogeneity has fundamental implications for adaptive phenotype fitness along environmental gradients. In this context, local adaptation may lead to population divergence and culminate in ecological speciation. In fact, ecological divergence of populations is a requirement for ecological speciation (Nosil, 2012; Schluter, 2009). Despite the growing literature on the role of local adaptation in population divergence, speciation and the evolution of reproductive isolation, few studies have inferred the role of gene expression in Neotropical systems (but see Leal et al., 2020, Raffini et al., 2020).

In Amazonian riparian forests, plant distribution is mainly determined by species' tolerance to waterlogging (Junk, 1989; Luize, Bauman, et al., 2024; Luize, Palma-Silva, et al., 2024; Wittmann et al., 2010). Also, contrasting environmental conditions, specially under small geographic scales might be an important factor in the divergence between populations of Amazonian trees (Brousseau et al., 2021). Moreover, examining genomic mechanisms is crucial for comprehending how plants adapt to the changing conditions within riparian ecosystems. Habitats and species are strongly affected by the Amazon basin flood pulse, addressing different wetland forest types (Junk et al., 2011; Luize, Bauman, et al., 2024; Luize, Palma-Silva, et al., 2024). It is therefore presumed that the Amazonian wetland forests represent linear refuges for species sensitive to waterlogging, from upland *Terra firme* riparian forests to clear-water floodplain forests (*Igapó*), one of the wetland typologies marginal to larger rivers (Junk et al., 2011). The increasing tolerance to the flooding gradient along the riparian zone, coupled with the high species turnover among streams and small rivers in riparian *Terra firme* forests (Schietti et al., 2014), can contribute to complementing regional diversity and structuring the distribution of species at the local scale. Thus, riparian vegetation total number of species varies according to soil water saturation, which decreases towards higher positions of the land (Gregory et al., 1991), and the flood pulse that modifies the environment quickly in time and space (Junk & Piedade, 1997). Notwithstanding, the response of biodiversity within Amazonian riparian forests to future climate and environmental changes will encompass not only shifts in species distribution but also in the intricate genomic mechanisms and pathways involved in environmental stress responses, especially in plants confronting varying flooding patterns—an aspect of knowledge that remains poorly understood in such habitats.

Ground-herbs, that is plants that spend their entire life cycle on the forest floor (Costa, 2004), commonly represent almost one third of the tropical forest total species diversity (Spicer et al., 2020). The distribution of ground-herb species changes along environmental gradients such as soil, water and light (Drucker et al., 2008). Among the neotropical herbs, Marantaceae is one of the most important families (Gentry & Emmons, 1987), predominating in Amazonian forest ecosystems (Costa, 2004; Duivenvoorden & Lips, 1995; Poulsen & Balslev, 1991). *Ischnosiphon puberulus* Loes. is a widespread Amazonian ground herb, from both primary and secondary forests, commonly growing in dense riverside shrubberies (Andersson, 1977). Details on its reproductive biology are unknown, but ants and crickets are likely effective seed dispersers (Santana et al., 2016). Understanding the adaptive responses of ground-herb species to environmental variation must provide crucial information on the evolution of the megadiverse Amazonian rainforest biota as well as new insights into key ecological functions affecting the distribution of Amazonian plants.

The interdisciplinary field of ecological genomics seeks to understand the genetic mechanisms underlying responses of organisms to their natural environments (Ungerer et al., 2008). Moreover, transcriptomics analysis provides a pathway towards a mechanistic understanding driving functional responses to natural environments and their genetic basis. Gene expression diversity is the ability of genes to modulate their expression levels, producing new phenotypes, without a necessary genetic change and may facilitate adaptation to environmental changes (López-Maury et al., 2008). Furthermore, in situ sampling of expressed genes, where the multivariate spectra of environmental gradients interact with the developing individual, promise to identify and characterize genes with

broad ecological and evolutionary relevance (Rivera et al., 2021). A comprehensive analysis of mechanisms through which species adapt and persist in stressful and changing habitats is crucial for the understanding and conservation of populations facing changing environmental conditions.

Here, we conducted a study on ecological transcriptomics of flooding regimes in the abundant ground-herb, *Ischnosiphon puberulus* (Marantaceae), a widely distributed species in the riparian zone of the Cupari River, in the Brazilian Amazon. We investigated natural populations of *I. puberulus* in two distinct types of Amazonian wetlands: floodplains with predictable, long-lasting, monomodal flood pulses in a clear-water river (i.e. *Igapó* forest), and wetlands subjected to short, unpredictable, polymodal flood pulses (i.e., *Terra firme* riparian forests) (Junk et al., 2011). We aimed to explore novel genetic insights into the molecular basis of environmental stress response in this tropical plant species. For that, we hypothesized that environmental differences (i.e. flooding lasting period, water column height and canopy openness) imposed by flooding regimes will promote differential gene expression responses between *I. puberulus* individuals from *Igapó* and *Terra firme* forests. We first predicted that transcripts differentially expressed between *Igapó* and *Terra firme* populations will be mostly linked with responses to abiotic stress (i.e. waterlogging, drought, and low light stresses). Thus, we would expect that populations adapted to floodplains have higher expression of genes related to stress response, mainly those involved in energetic balance, water transport and hormones, as compared to small stream riparian populations. Second, we predict that environmental differences will be associated with genetic differences, indicating that isolation by environment, rather than isolation by distance, is the primary driver of genetic differentiation between *Igapó* and *Terra firme* riparian populations. If these predictions are corroborated, we expect to identify locally adapted genes associated with divergent environments.

To accomplish this, we characterized the environments where samples were taken and also assembled and annotated a reference chromosome-level genome for the species, based on PacBio and Omni-C reads. Using this reference genome, we analysed transcriptomes of individuals of *I. puberulus* from *Igapó* and *Terra firme*, aiming to identify genes under differential expression as well as to reveal contrasting patterns of genetic differentiation between *Igapó* and *Terra firme* individuals.

2 | MATERIALS AND METHODS

2.1 | Study area

We conducted this study in the Brazilian national sustainable use protected area Tapajós National Forest (TNF), located on the right bank of the Tapajós River, Brazilian Amazon (−4.022310 to −3.744208° S, −54.921920 to −55.392877° W, ICMBio 2014). TNF covers 527,319 hectares (Soares, 2004) and is mostly vegetated by evergreen rainforest (Veloso et al., 1991) over Dystrophic Yellow Latosols, deep soils with low cation exchange capacity (Hernandez et al. 1993). The Cupari River is a right tributary of the lower Tapajós River, with part of its basin located in the TNF area (Figure 1). Cupari River basin has 721,620 ha and its area belongs to the tropical rainy climate with annual thermal variation below 5°C. According to Köppen-Geiger's climatic classification, its typology is *"Am"*, or rather, tropical monsoon climate, with a dry season and intense rains for the rest of the year. The mean annual rainfall is 1820 mm, with great variation along the year and higher precipitation records

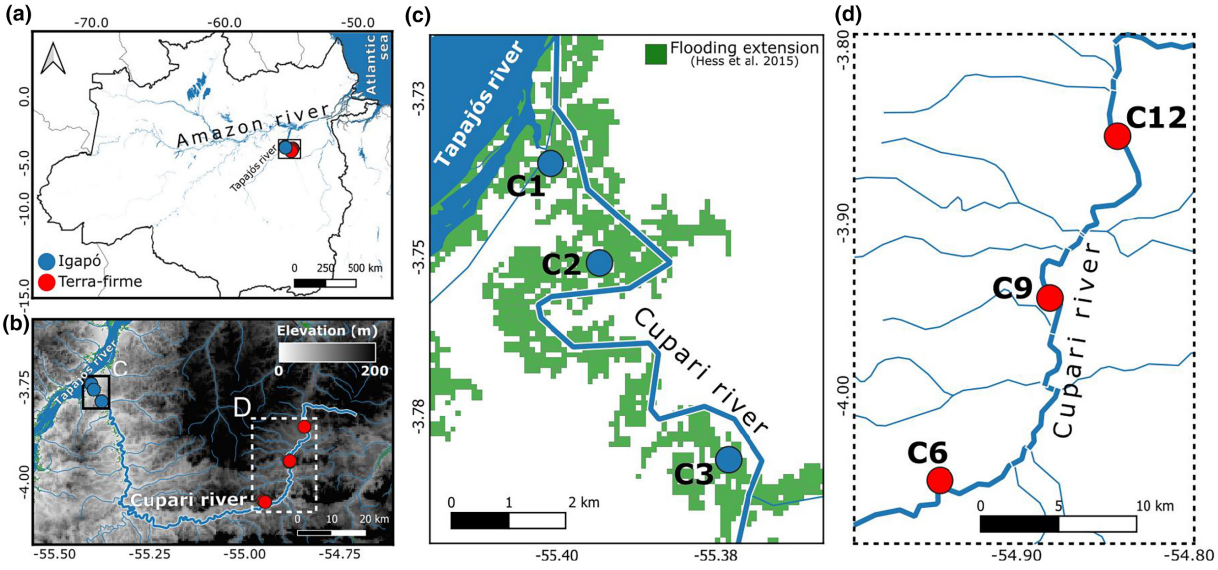

FIGURE 1 Population sampling of *Ischnosiphon puberulus*. Sampling sites within the Amazon River basin (a) and the Tapajós sub-basin (b). Sampling *Igapó* and *Terra firme* areas are indicated in blue (c) and red (d), respectively. Elevation deficits are represented by a black and white gradient in b and flooding extension as green coloured areas in c.

from January to May (Soares, 2004). Tributaries usually draining Ferralsols often present transparent, crystalline waters (Herrera et al., 1978), as the Cupari River.

2.2 | Environmental variables

To characterize the sampling sites of *I. puberulus* (Figure 1), we set six 250 m long riparian plots along the Cupari basin within the TNF. Sampling was carried out monthly from November 2018 to January 2020. Sample site locations within the watershed were randomly selected considering at least 1 km minimum distance (linear and hydrographic) between each other. Sampling sites were installed in *Terra firme* (C6, C9 and C12) and *Igapó* (C1, C2 and C3) forests, the former was represented by riparian forests of small order streams and the latest by the Cupari River main channel, to capture natural environmental changes throughout the fluvial waterlog.

Flooding parameters were measured with a hydrological station to sample monthly river level data at each riparian site. We recorded the water column height (i.e. the vertical distance from the bottom of the river/stream and the flowing water) and the flooding duration (i.e. the number of months with waterlogged soil). We used one limnimetric ruler per site to record river level, which were installed in the dry season and sampled monthly from December 2018 to January 2020. Limnimetric rulers were 3 m high, graduated at each 10 cm, and positioned at the margin and the bottom of the river/stream channels. Its exact position was marked with coloured tape on tree trunks, and GPS coordinates were taken to enable the measurements during the flood period, when the rulers at the larger river sites were submerged. For such cases, we used an anchor-like device attached to a rope to estimate river/stream depth at the same point of the ruler. For the water column height (cm), we used the maximum value of each riparian sampled site, and for flooding duration (number of months), we used the total number of months with waterlogged soil at the sampling site. We assumed that *Igapó* sites would present highest values for both variables, given their lower position in the terrain, compared to *Terra firme* sites.

Canopy openness (%) was estimated from plan digital photographs taken during the wet season between November and December 2019. On each site (C1, C2, C3, C6, C9 and C12), a 250 m line positioned parallel to the adjacent water body (stream or river) was marked every 50 m (0, 50, 100, 150, 200, 250 m), summing six canopy openness subsamples per site. Subsamples consist of four photos taken perpendicularly to the forest canopy, at 2 m high from the ground, at north, south, east and west directions, with a Nikon® Af-s Nikkor® 35 mm lens. Each site canopy openness information was composed by four photos from six subsamples, summing 24 digital photographs per site. Each photograph was converted to monochromatic (black and white) images using an image editor (Adobe® Photoshop® CS6), and canopy openness percentage was calculated as the mean of the proportion of white pixels from the total amount of pixels per image (Bleich et al., 2014).

2.3 | High quality genome sequencing

For PacBio HiFi sequencing, young leaf tissue of a single individual of *I. puberulus* sampled in *Igapó* population C3 was sent to Arizona Genomics Institute (The University of Arizona, USA). Total genomic DNA was extracted from this sample using the cetyl trimethylammonium bromide method (CTAB) (Doyle & Doyle, 1987). A whole-genome shotgun sequencing library was prepared with SMRTbell Express Template Prep Kit 2.0 (Pacific Biosciences, Menlo Park, CA), including DNA fragmentation, DNA damage repair and end repair, hairpin adapter ligation and DNA purification. Long-read High fidelity—HiFi—sequencing was performed on a Sequel IIe in circular consensus sequencing (CSS) mode, producing 15.6 Gb of HiFi sequence data.

To help with the phasing of the genome and with the scaffolding, we also generated high-resolution chromatin conformation capture (Hi-C) using the Omni-C kit for this individual. The Dovetail Omni-C library was constructed and sequenced by Arizona Genomics Institute (The University of Arizona, USA) by using standard protocols (Dovetail Genomics, Dovetail Omni-C Kit Catalogue #21005). One gram of flash-frozen leaf tissue of the same *I. puberulus* individual was ground using a SPEX Sample Prep Freezer Mill. Nuclei isolation was performed using the Circulomics LN2 Plant Tissue Protocol (Circulomics NUC-LNP-001). The nuclei pellet was resuspended in 1X PBS, aliquoted into three tubes and centrifuged at 6000 rpm for 5 min. The supernatant was then discarded and the nuclei pellets flash frozen for storage at −80°C. One aliquoted nuclei pellet was then processed using the mammalian cell protocol with Dovetail Omni-C protocol mammals V1.3. Completed libraries were sequenced on an Illumina NovaSeq 6000 PE150.

2.4 | Chromosome-level genome assembly

Prior to assembly procedures, we evaluated the quality of the raw PacBio data with Blobtools v1.1.1 (Laetsch & Blaxter, 2017) and genome size and heterozygosity was investigated with GenomeScope2 and SmudgePlots v0.2.3 (Vurture et al., 2017). We used the software Hifiasm v0.19.7-r598 (Cheng et al., 2021) to assemble a phased genome with the PacBio HiFi and Omni-C reads. Scaffolding of each haplophased assembly was performed with YAHS (Zhou et al., 2023), followed by manual curation with PretextView v0.2.5 (Howe et al., 2021). Genome assembly accuracy and completeness was assessed for each phased haplotype with Quast v5.0.2 (Gurevich et al., 2013), BUSCO v5.0 (Manni et al., 2021) and Merqury v1.3 (Rhie et al., 2020).

2.5 | Gene prediction and structural annotation

Genome annotation was carried out using the haplophase 1, due to higher completeness-related assembly summary statistics, evaluated by Quast (Gurevich et al., 2013). The identification of repetitive regions and masking of genome assembly of *I. puberulus* was performed

with RepeatModeler v2.0.3 (Flynn et al., 2020) and RepeatMasker v4.1.1 (Tarailo-Graovac & Chen, 2009), using the soft-masking option (-xsmall). RNA-seq data of two individuals per sampled population of *I. puberulus* (see below) was used in the aid of the genome annotation. We used BBMap (Bushnell, 2014) to align the RNA-seq reads against the genome. The structural annotation was then carried out with the BRAKER2 pipeline (Brůna et al., 2021), following the "Braker with RNA-seq data" pipeline mode, using the aligned RNA-seq data as extrinsic evidence. The annotation was done using the genome files containing the 13 largest scaffolds (pseudomolecules) on the *I. puberulus*' genome. Gene density, protein-coding sequence content and also the GC content were then plotted into a Circosplot with the R package circlize (Gu et al., 2014), to better visualize the genomic features that were found and annotated.

2.6 | Population sampling and RNA extraction

We conducted RNA-seq analysis to characterize differential expression and infer patterns of genetic differentiation in 41 individuals of *Ischnosiphon puberulus* collected under two antagonist and stressful conditions: periodically flooded forests *Igapó* (three sites) and mostly non-flooded forest *Terra firme* (three sites) (Figure 1) during the end of the dry season (december 2021). Leaf samples were collected in RNAlater solution (Thermo Fisher Scientific, USA) at room temperature and subsequently stored at −80°C until RNA extraction. Each sample was georeferenced and one voucher was deposited in the HSTM herbarium (M.A.Buitrago 472). Total RNA was extracted from fresh leaves using a QIAGEN RNeasy® Plant Mini Kit (Qiagen, Finland). We used agarose gel 1% stained with gel-red (Biotium Inc., USA) to check the quality and integrity of extracted RNA, and further quantified the samples using Qubit4 fluorometer Invitrogen (Thermo Fisher Scientific, USA). Samples were sent to Macrogen Inc. (South Korea) to perform the total RNA library construction using TruSeq stranded mRNA library kit. Paired-end sequencing was performed on the Illumina NovaSeq 6000 platform (pair-end reads of 100 pb ~50 M reads per sample).

2.7 | Transcriptome assembly and annotation

We examined quality metrics from the Illumina paired-end raw reads using FastQC (https://www.bioinformatics.babraham.ac.uk/projects/fastqc/). We then corrected erroneous k-mers from reads using Rcorrector v1.0.4 (Song & Florea, 2015) with default settings and removed reads with unfixable errors using TranscriptomeAssemblyTools (https://github.com/harvardinformatics/TranscriptomeAssemblyTools). After trimming adaptors and low-quality bases using TrimGalore v.0.6.0 (http://www.bioinformatics.babraham.ac.uk/projects), we removed ribosomal RNA listed in the SILVA database (Quast et al., 2012) using the bbduk.sh script from the BBMap package v38.90 (https://jgi.doe.gov/data-and-tools/bbtools/).

Filtered reads from a subset of 12 samples (two samples per population) were further used to perform the de novo assembly of a reference transcriptome guided by the haplophase 1 of the reference genome of *I. puberulus* using Trinity v2.8.5 (Grabherr et al., 2011; Haas et al., 2013). For this, we aligned the filtered reads against the species' genome using STAR v2.7.9 (Dobin & Gingeras, 2015), then merged the individual BAM files and sorted the coordinates using SAMtools v.1.10 (Danecek et al., 2021). We ran the genome-guided de novo assembly in Trinity by setting the maximum intron length to 1000 bp. General assembly statistics were obtained with TrinityStats.pl script. We assessed the completeness of the transcriptome by aligning assemblies against the Viridiplantae IPG database and tested for the benchmarking universal single-copy ortholog (BUSCO) content (Simão et al., 2015).

We carried out the functional annotation of the reference transcriptome using OmicsBox v3.0.30 (BioBam, Valencia, Spain) (Götz et al., 2008) platform. For this, we filtered for contigs longer than 300 bp and aligned them against the NCBI non-redundant NR protein database for Viridiplantae with an e-value cut-off of 10e−5. We also used the InterProScan (Zdobnov & Apweiler, 2001) to retrieve protein domains and the Kyoto Encyclopedia of Genes and Genomes (KEGG) to obtain the attribution of Enzyme Commission (EC) terms and metabolic pathways.

2.8 | Differential expression analysis

We compared the patterns of gene expression between *I. puberulus* samples from *Terra firme* and *Igapó* sites following the Trinity pipeline. To do so, we mapped filtered reads to the reference transcriptome using Bowtie 2 and summarized read counts of each of the 41 samples as implemented in the RSEM 2.01 software (Li & Dewey, 2011). Then, we used the Trinity script run_DE_analysis.pl to perform the differential expression analysis at transcript level based on the isoform count matrix with edgeR R-package (Robinson et al., 2010) by setting a false discovery rate (FDR) cut-off of 0.001 and a minimum of four-fold expression change. We further clustered all differentially expressed transcripts according to the patterns of differential expression using a matrix of FPKM values computed from TMM normalization of the isoform count matrix. A GO enrichment analysis was used to infer over-represented biological processes among the differentially expressed transcripts (DETs) between *Terra firme* and *Igapó* using the R-package topGO (Alexa & Rahnenfuhrer, 2010) by setting the Elim–Kolmogorov–Smirnov method with a significance threshold of 0.01. To exclude redundant terms (semantic similarity >0.7) and summarize information coming from the enriched GO terms, we performed a semantic analysis implemented in the REVIGO Web server (Supek et al., 2011).

2.9 | SNP calling

Filtered RNA-Seq reads were mapped on the haplophase 1 reference genome of *I. puberulus* using a two-pass procedure in STAR v2.7.9

(Dobin & Gingeras, 2015) for robust and accurate variant discovery. We performed the 1-pass STAR mapping, then used the splice junctions obtained during the 1-pass to re-generate the genome indices to run the 2-pass step mapping. Following the workflow of the Genome Analysis Toolkit v4.2.0.0 (GATK; DePristo et al., 2011; Van der Auwera et al., 2013) for RNAseq short variant discovery, we marked duplicate reads and added read groups using Picard (http://broadinstitute.github.io/picard). We then used SplitNCigarReads tool to split reads into exon segments (getting rid of Ns but maintaining grouping information) and hard-clip any sequences overhanging into the intronic regions. The GATK module 'HaplotypeCaller' was used to call genotypes for each sample; then, 'GenomicsDBImport' and 'GenotypeGVCFs' GATK modules were used to call variants among samples. We filtered out SNP clusters (i.e. three or more SNPs in a sliding window of 35 pb) and any variant with Fisher strand (FS) values < 30.0 and quality by depth (QD) < 2.0 using the 'VariantFiltration' GATK module. We also used VCFtools v0.1.17 (Danecek et al., 2011) to retain only biallelic SNPs, with minimum read depth of 10, minimum allele frequency of 2% and maximum of 10% missing individuals. We excluded four out of 41 individuals with more than 10% missing data to obtain the full dataset. A thinned dataset was further generated by subsampling one SNP per window of 10,000 bp using VCFtools to perform the genetic structure analysis, which requires non-linked loci, and estimate population-level genetic diversity.

2.10 | Population genetic analyses

We inferred patterns of genetic structure from SNPs dataset in *I. puberulus* using a Bayesian analysis implemented in the software Structure v2.3.4 (Falush et al., 2003; Pritchard et al., 2000). Structure was run under the admixture model allowing for correlated allele frequencies, using a burn-in of 100,000 followed by 500,000 Markov Chain Monte Carlo (MCMC) iterations. Ten replicate runs were performed for each value of K (number of clusters) ranging from one to seven and the best K was inferred by Structure Harvester v0.6.94 (Earl & VonHoldt, 2012). The individual admixture proportions for the best K averaged across runs was visualized with CLUMPAK (Kopelman et al., 2015).

To compare within-site genetic diversity between *Igapó* and *Terra firme* sites, we calculated allelic richness, observed (H_O) and expected (H_E) heterozygosities, and inbreeding coefficient (F_{IS}) with their confidence intervals based on 100 bootstrap using the R packages 'diveRsity' (Keenan et al., 2013), 'PopGenKit' (Paquette & Paquette, 2011) and 'hierfstat' (Goudet, 2005). We also estimated the genetic differentiation among sites using pairwise F_{ST} values as calculated by R-package 'hierfstat'.

2.11 | Environmental correlates of genetic differentiation

We performed Mantel tests on the genetic differentiation in *I. puberulus* to test for the relative effects of isolation by distance (IBD) and isolation by environment (IBE). To do so, we calculated pairwise F_{ST} among sampled sites using R package 'PopGenKit', then linearized the values as $F_{ST}/(1-F_{ST})$ (genetic differentiation matrix). We also calculated pairwise geographical distances from the sites coordinates (geographical matrix) and pairwise Euclidean environmental distances based on the per-site water column maximum height, flooding period and canopy openness in conjunction or independently (four distinct environmental matrices) using the 'vegdist' function in R package 'vegan' (Oksanen et al., 2022). As sampling sites follow a bimodal distribution, we ran each Mantel test using Spearman correlation and tested for their significance using 1000 permutations with 'vegan'. We also used a partial Mantel to evaluate the effect of the environmental distance on the genetic differentiation controlling for the geographical distance using 'vegan' based on the Spearman correlation.

3 | RESULTS

3.1 | Environmental variables

Sampling sites vary in terms of the environmental variables accessed (water column height, flooding duration and canopy openness percentage), mostly because of the position in the drainage system (Figure 1). While *Igapós* forests sites remained submerged for up to 8 months, the *Terra firme* riparian forests sites remained submerged for a maximum of 3 months (Table S1). Variation was even greater in the height of the water column; as the *Terra firme* sites varied much more among themselves than the *Igapó* sampling sites. While the maximum water column height in *Igapós* varied approximately between 6.8 and 8.1 m, such variation on *Terra firme* was between 0.18 and 1.8 m (Table S1). The site C12 had 0.18 m of maximum water column height, being characterized as a small headwater stream, and its influence on the soil and adjacent vegetation should be more discreet, compared to the other sites. Although canopy opening also varied between sites, it was dense in all of them (minimum of 5% and maximum of 12% of opening, see Table S1). Nevertheless, the *Igapó* forest sites showed greater canopy openness variation between sites than the *Terra firme* forest sites.

3.2 | Genome assembly and structural annotation

We generated a total of 15.6 Gb of HiFi sequence data (~49× coverage) and 43.6 Gbp of OmniC data (~133× coverage) to assemble the genome. The SmudgePlot analysis indicates the species is diploid. The high-quality chromosome-level phased genome assembly for *Ischnosiphon puberulus* produced a genome size of 328 Mbp for haplophase 1 and 341 Mbp for haplophase 2 (Figure 2). After scaffolding and manual curation, we obtained a total of 81 and 74 scaffolds for haplophase 1 and 2, respectively, and 13 large scaffolds for each haplophase, which is consistent with the chromosome number reported for the congeneric

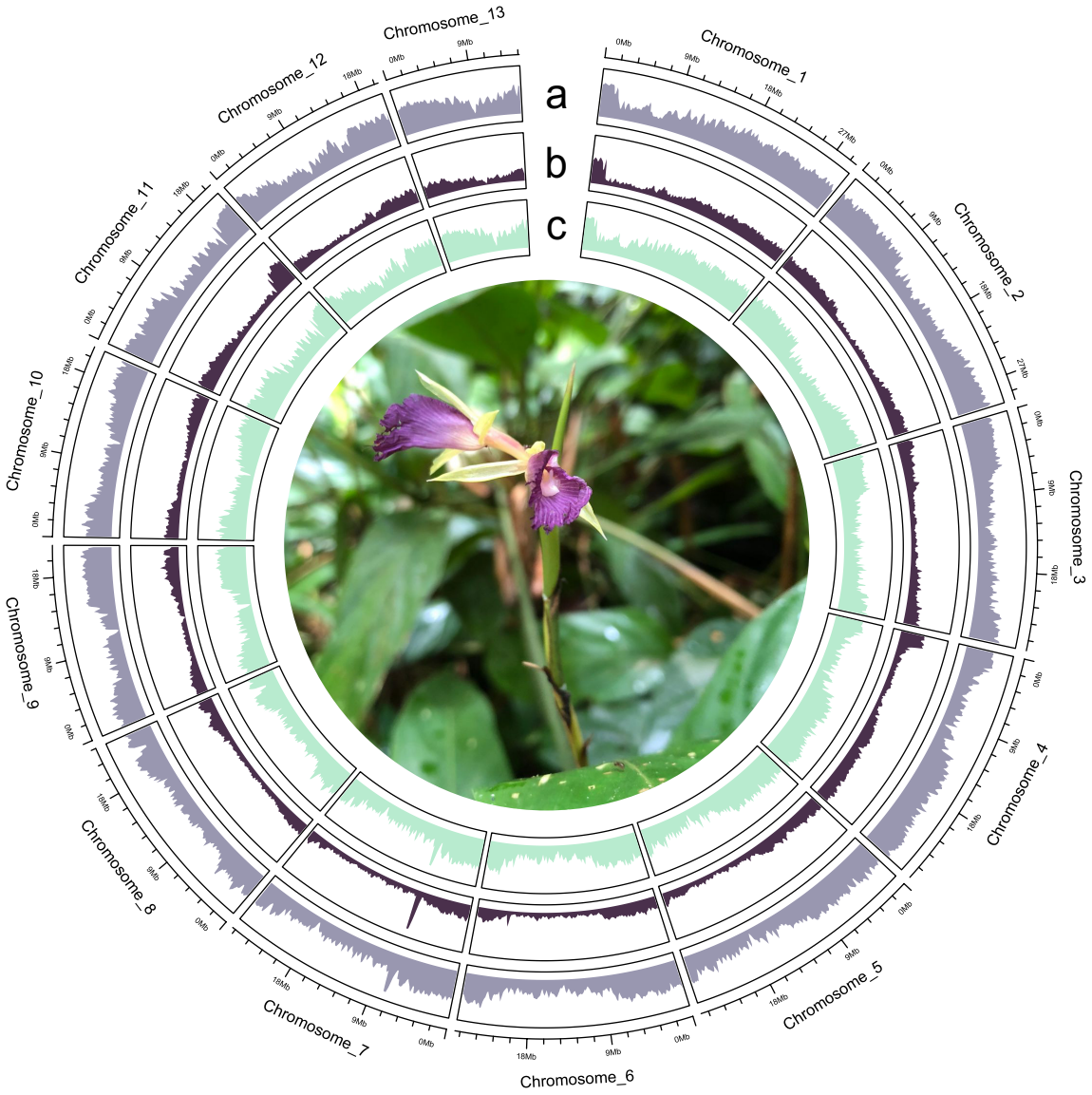

FIGURE 2 Circosplot of *Ischnosiphon puberulus* genomic features in each chromosome. (a) Gene density, (b) GC content along the genome and (c) protein-coding sequence density.

species *I. leucophaeus* ($2n = 26$, Santos et al., 2022). The size of each pseudomolecule varied from ~14 to ~30 Mb, with telomeric repeats in one or both ends. The *I. puberulus* genome showed a N50 of 25.5 Mb and ~ 99% of orthologous genes were found in the Embryophyta ortholog database v10. Merqury analysis indicated a completeness of >83% for both haplophases separately and 99.43% when analysed together. The structural annotation indicates that 49.16% of *I. puberulus* genome is composed of repetitive elements. A total of 60,471 protein coding genes were detected on *I. puberulus*' 13 scaffolds (haplophase 1), with 4.92 exons per gene and an average gene length of 2717.77 bp. We found a higher density of genes and protein-coding sequences near the telomeric regions on most *I. puberulus* chromosomes (Figure 2). The same pattern was observed for GC content, which showed higher abundance near chromosomes' ends rather than near the centromeric regions (Figure 2). Assemblies and underlying raw sequencing data were deposited on NCBI under BioProject PRJNA1055542.

3.3 | Transcriptome assembly and functional annotation

The assembled reference transcriptome had a total of 139,637 contigs, of which 103,398 contigs were longer than 300 pb (average contig length = 1299.53 pb, N50 = 1709 pb), after removing redundant (100% identity) contigs, and one contig from viral origin, 102,727 contigs remained for further analyses. According to the BUSCO analysis, 94.2% of the genes were complete, while fragmented and missing genes corresponded to only 3% and 2.9%, respectively. We annotated gene ontology (GO) terms for ca. 49.6% of the contigs (50,885 out of 102,727).

3.4 | Differential gene expression patterns

Samples from contrasting flooding conditions (*Terra firme* vs. *Igapó*) were well differentiated by their gene expression profiles (Figure 3a). Gene expression analysis identified a total of 4326 differentially expressed transcripts (DETs) between such environments out of a total 68,387 identified transcripts. Among these, 1948 were upregulated in *Igapó* (Figure 3b; Table S2) and 2309 were upregulated in *Terra firme* (Figure 3c; Table S3). The analysis implemented in topGO pointed to 29 non-redundant GO-terms significantly enriched for this comparison ($p < .01$) (Table 1). These GO-terms are associated with an array of biological functions. The most significant enriched GO terms between *Terra Fime* and *Igapó* were defence response, water transport, phosphorylation, root development, response to auxin, responses to oxidative stress and responses to salicylic acid (Table 1), which are known to represent universal components in responses to abiotic stresses responses (i.e., waterlogging, drought, UV-radiation, etc) in plants (Gupta et al., 2016; Mittler, 2006; Roelofs et al., 2008).

Several genes involved in plant protection by signalling the activation of stress response were differentially expressed in this study. For instance, ~40 DETs between *Igapó* and *Terra firme* are putative cytochrome P450 (CYP) enzymes: cytochrome P450, flavonoid 3′-monooxygenase (CYP75B137-like; EC: 1.14.14.82), flavin-containing monooxygenase (EC: 1.14.13.8), flavonoid 3′,5′-hydroxylase (EC 1.14.14.81), flavanone 3-dioxygenase, abscisic acid 8′-hydroxylase (CYP707A1; EC 1.14.14.137) and protein LUTEIN DEFICIENT 5 (EC: 1.14.14.158). Likewise, ~30 DETs were identified as potential thioredoxins and glutaredoxins and its associated enzymes: Thioredoxin-disulfide reductase, thioredoxin family protein, thioredoxin H2-2, thioredoxin superfamily protein, thioredoxin-like 1–2, thioredoxin-like protein AAED1, thiol-disulfide oxidoreductase LTO1, ferredoxin-thioredoxin reductase catalytic chain, monothiol glutaredoxin-S6, glutaredoxin family protein, glutaredoxin-C8-like, glutathione S-transferase, glutathione synthetase and ascorbate transporter.

Other genes were upregulated only in *Igapó*: DELLA gene family plays key roles in regulating plant development and stress response (Luo et al., 2023); early light-induced protein 1 (ELIP); drought-induced protein 1; protein LOW PSII ACCUMULATION 1; RuBisCO large subunit-binding protein subunit alpha; superoxide dismutase [Fe] 2; and chlorophyll(ide) b reductase NYC1 (EC 1.1.1.294) (Table S2). Some genes were overexpressed only in *Terra firme* populations, such as monodehydroascorbate reductase (EC:1.6.5.4), EID1-like F-box protein 3, heat shock cognate 70 kDa protein 2, aquaporin TIP4-3, protein YELLOW LEAF 1, phytochromobilin: ferredoxin oxidoreductase, enolase 2 (EC:2.7.11.17) (Table S3).

Our gene expression analysis detected a third cluster of 68 DETs upregulated in individuals from the *Terra firme* C12 population, when compared to other individuals from *Terra firme* (C6 and C9) or those from *Igapó* (C1-C3, Figure 3d). These are significantly

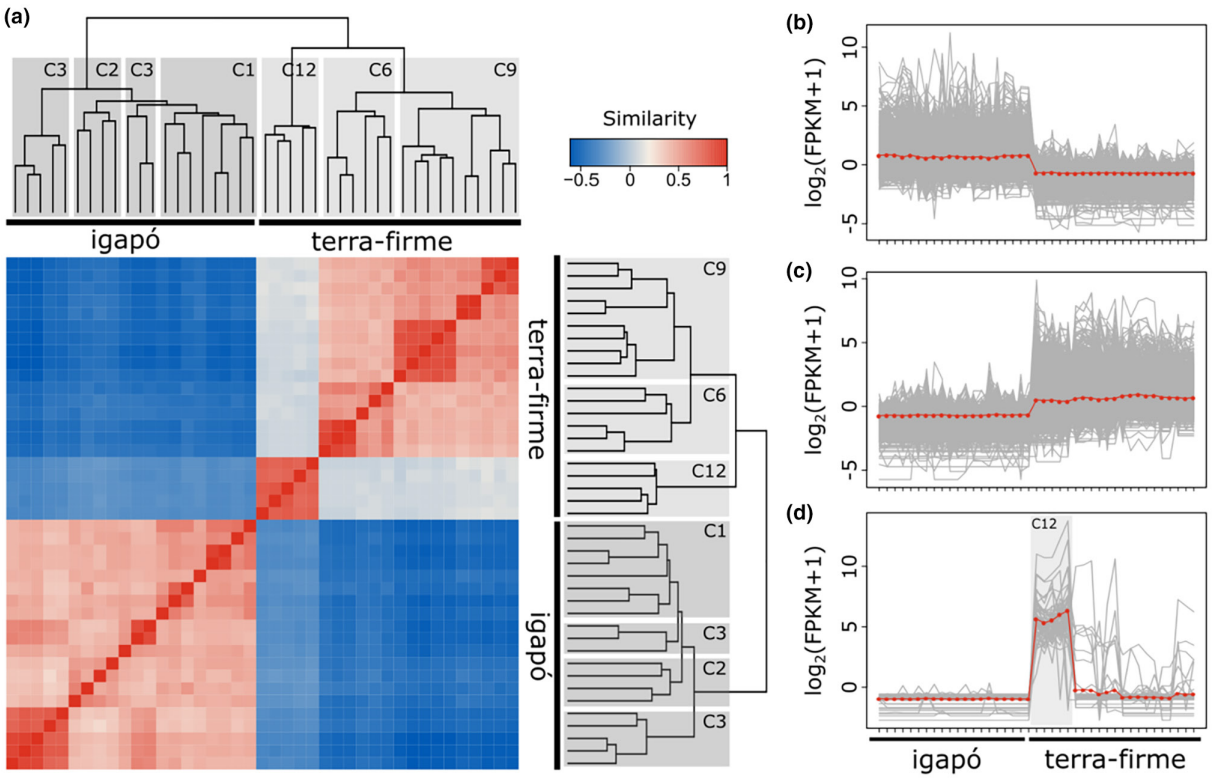

FIGURE 3 Gene expression patterns between *Ischnosiphon puberulus* sampled in *Terra firme* and *Igapó*. Sample correlation matrix heatmap for 4326 differentially expressed transcripts (a). Expression levels of the subsets of genes upregulated in the *Igapó* (=1948, in b), *Terra firme* (=2309, in c) and C12 population (=68, in d).

TABLE 1 Non-redundant enriched GO-terms in the comparison among differentially expressed transcripts of *Terra firme* and *Igapó* samples of *Ischnosiphon puberulus*.

GO term	Name	Log (*p*-value)	Log (size)	Frequency	Uniqueness	Dispensability
GO:0006952	**Defence response**	**−2.123**	**3.202**	**7.383**	**0.878**	**0.440**
GO:0016310	**Phosphorylation**	**−4.503**	**3.143**	**6.437**	**0.775**	**0.449**
GO:0048364	**Root development**	**−2.091**	**2.742**	**2.555**	**0.939**	**0.312**
GO:0009733	**Response to auxin**	**−2.259**	**2.656**	**2.096**	**0.873**	**0.469**
GO:0006979	**Response to oxidative stress**	**−4.441**	**2.640**	**2.022**	**0.889**	**0.000**
GO:0009751	**Response to salicylic acid**	**−2.697**	**2.246**	**0.811**	**0.881**	**0.313**
GO:0034219	Carbohydrate transmembrane transport	−2.199	1.897	0.361	0.808	0.434
GO:0010090	Trichome morphogenesis	−2.003	1.806	0.292	0.896	0.449
GO:1990961	Xenobiotic detoxification by transmembrane export across the plasma membrane	−2.843	1.708	0.232	0.737	0.170
GO:0006833	Water transport	−2.061	1.602	0.181	0.863	0.364
GO:0009395	Phospholipid catabolic process	−2.672	1.362	0.102	0.704	0.078
GO:0009147	Pyrimidine nucleoside triphosphate metabolic process	−2.605	1.342	0.097	0.716	0.502
GO:0042938	Dipeptide transport	−2.394	1.279	0.083	0.859	0.277
GO:0001731	Formation of translation preinitiation complex	−3.062	1.079	0.051	0.853	0.000
GO:0010199	Organ boundary specification between lateral organs and the meristem	−2.155	1.000	0.042	0.932	0.000
GO:0043631	RNA polyadenylation	−2.131	0.845	0.028	0.879	0.141
GO:0072488	Ammonium transmembrane transport	−2.448	0.845	0.028	0.826	0.437
GO:1990547	Mitochondrial phosphate ion transmembrane transport	−2.466	0.602	0.014	0.842	0.340
GO:0000957	Mitochondrial RNA catabolic process	−2.189	0.477	0.009	0.830	0.411
GO:0097510	Base-excision repair, AP site formation via deaminated base removal	−2.233	0.301	0.005	0.826	0.206

Note: In bold are the top significant enriched GO term between *Terra fime* and *Igapó*.

enriched for 25 non-redundant GO-terms linked to diverse metabolic processes and to putative adaptive processes, such as water transport, defence response and response to oxidative stress (Table S4).

3.5 | Genetic diversity and population differentiation

After calling and filtering SNPs using the GATK workflow, we obtained a total of 65,472 high-quality transcriptome-derived SNPs (full dataset). The additional filtering step used to retain unlinked loci from the full dataset resulted in 7,387 SNPs (thinned dataset).

Structure bayesian analysis revealed three well-defined clusters based on the thinned dataset; the first formed by samples from the three *Igapó* populations, the second formed by samples from two *Terra firme* populations (i.e. C6 and C9) and the third represented by C12 *Terra firme* population (Figure 4a). The analysis showed no pattern of admixture in the codifying part of the genome among these clusters. The pairwise genetic differentiation between *Igapó* and *Terra firme* populations also evidences this differentiation by the highest F_{ST} values among populations from distinct flooding conditions (F_{ST}=0.250–0.422), than those from the same flooding condition (F_{ST}=0.091–0.122), with exception of C12, which was highly differentiated from all other populations (F_{ST}=0.373–0.422; Table S5).

Levels of genetic diversity were similar in *Terra firme* and *Igapó* populations, with exception of C12, which showed slightly lower observed and expected heterozygosities (Figure 4b, Table S6). Although not significant, the allelic richness was also lower in C12 than in the remaining populations. Inbreeding coefficients were negative for all analysed populations due to the excess of heterozygotes, with no consistent differences between *Terra firme* and *Igapó* (Figure 4b, Table S5).

3.6 | Environmental correlates of genetic differentiation

We detected no significant correlation between population genetic differentiation ($F_{ST}/(1-F_{ST})$) and geographical distances (Mantel r=.236, p=.139), indicating the absence of isolation-by-distance among *I. puberulus* populations. The correlation between genetic differentiation and environmental distance, as

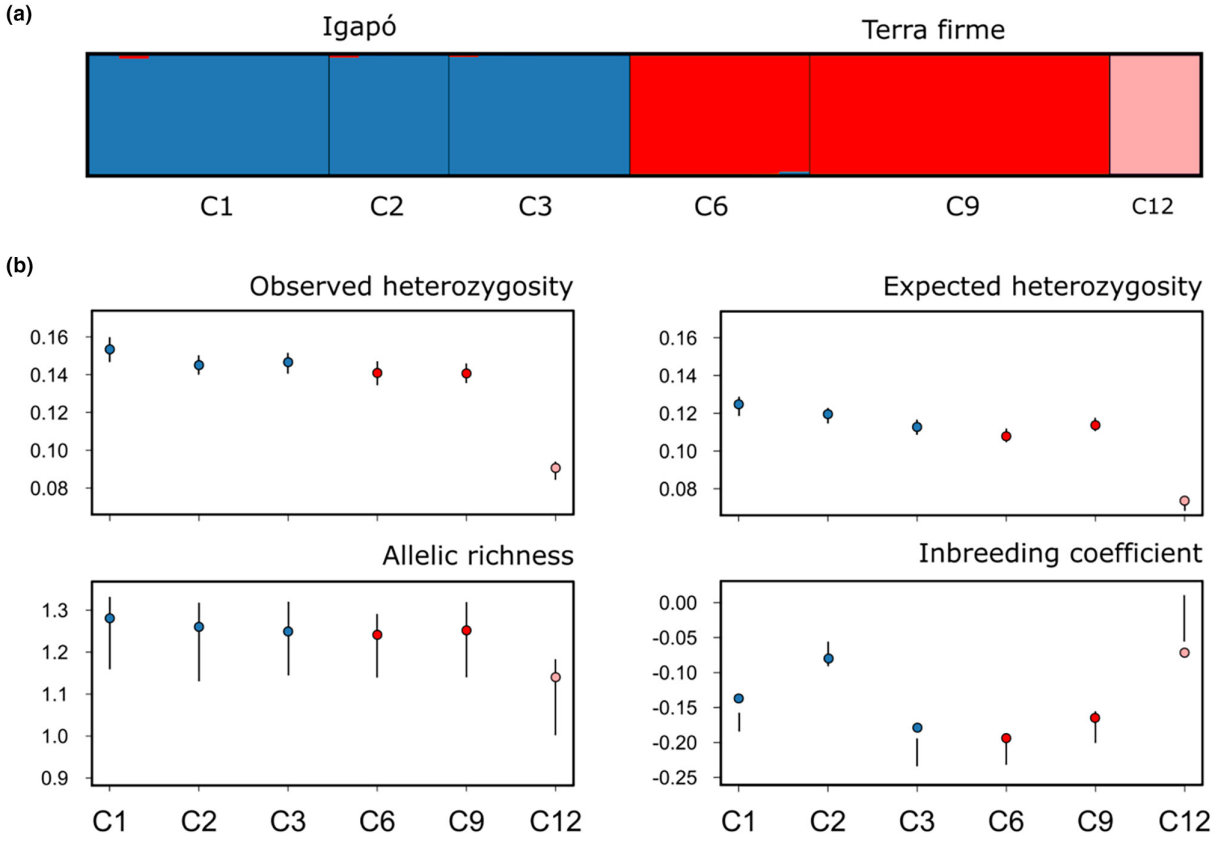

FIGURE 4 Population genetic structure and genetic diversity per population of *Ischnosiphon puberulus*. Bar plot depicting the Structure clustering analysis for $K=3$ based on 7387 transcriptome-derived SNPs sampled in six populations from either *Igapó* or *Terra firme* (a). Mean estimates and 95% confidence intervals of observed and expected heterozygosity, allelic richness and inbreeding coefficient, per population (b).

determined by the variation of the three environmental variables in conjunction, suggests a trend towards significance (Mantel $r=.336$, $p=.055$). In fact, when testing each environmental variable separately, mantel tests indicate weak and non-significant correlation between genetic differentiation and canopy openness or flooding period. On the other hand, population genetic differentiation and water column height was strongly and significantly correlated (Mantel $r=.582$, $p=.015$), suggesting that genetic variation was better explained by the effect of isolation-by-environment. When we controlled for the geographical distance, such a relationship remained strong although not significant (Partial Mantel $r=.621$, $p=.068$).

4 | DISCUSSION

Here we showed that gene expression profiles were well differentiated between populations from the *Igapó* and *Terra firme* forests (Figure 3a). Moreover, differentiation in gene expression was highly congruent with population genetic divergence between *Igapó* and *Terra firme* (Figure 4a). The presence of isolation by environment suggests that environmental differences, such as water column height, serve as the primary drivers of population differentiation and gene expression patterns. Indeed, seasonal waterlogging is one of the most prominent environmental challenges in *Igapó* compared to *Terra firme* environments (Parolin et al., 2004). In agreement, here we observed environmental contrasts between *Igapó* and *Terra firme* were evidenced by the great differences in water column height and duration of flooding periods. Our results suggest that environmental differences imposed by flooding regimes promoted population genetic differentiation and differential transcript expression responses in *I. puberulus* individuals from *Igapó* and *Terra firme* forests. Furthermore, enriched GO terms revealed that most differentially expressed genes were associated with abiotic stress: defence response, water transport, phosphorylation, root development, response to auxin, responses to oxidative stress and responses to salicylic acid (Table 1). Our data not only informed us about the genetic structure of *I. puberulus* populations but also provided important information about the environmental variables that may be responsible for the divergent gene expression maintaining the observed genetic structure.

Among enriched GO terms, we found several differential expressed transcripts associated with cytochrome P450 (CYP) genes and thioredoxins and glutaredoxins antioxidant systems. CYPs are versatile enzymes involved in numerous biological processes of plant growth and development, and they play a crucial role in plant protection by signalling the activation of stress response (Pandian et al., 2020). Thioredoxins and glutaredoxins are also

involved in plant growth and development as well in protecting plants from oxidative damages caused by abiotic stresses (Meyer et al., 2012). Abiotic stresses typically induce oxidative damage as a consequence of increased production of reactive oxygen species (ROS). As mitochondria and chloroplasts are the main cellular compartments that experience oxidative burst when plants face stressful conditions (Blokhina et al., 2003), we may argue that enriched GO terms and DTE analyses may have revealed differences in respiration and photosynthesis between *Terra firme* and *Igapó* populations. Anoxia (deficiency of oxygen) is a primary effect of waterlogging (Ashraf, 2012) already well documented for Amazonian trees (Piedade et al., 2010). As plants face excessive energetic pressure on primary photochemistry and have reduced energy production through respiration under oxygen deprivation, an effective antioxidant defence systems is needed to limit oxidative damage and enhance the stress resistance of plants, avoiding lipid peroxidation, oxidation of proteins, enzyme inhibition and injury to DNA/RNA (Hasanuzzaman et al., 2017).

The putative cytochrome P450 (CYP) genes identified in this study likely play a pivotal role in the environmental stress response of plants in both *Igapó* and *Terra firme* populations and suggest that these plants may have the ability to detoxify the adverse effects of ROS by producing a range of antioxidants. In plants, cytochrome P450 belongs to a large family of genes with numerous functions in many important cellular processes, which are crucial to plant resilience under abiotic stress (Hansen et al., 2021). The expression of various CYP genes is regulated in response to abiotic stress and plays a central role in regulating anaerobic metabolism, detoxification and hormone signalling pathways (Renault et al., 2014). Their involvement in flavonoid metabolism, abscisic acid signalling and other stress-related pathways indicate their role in plant adaptation strategies (Hansen et al., 2021; Pandian et al., 2020). Flavonoids are known to play an essential role in stress mitigation, acting as antioxidants and signalling molecules and protecting plants from oxidative damage induced by drought, salt, cold, UV-radiation and heavy metals (Shomali et al., 2022). In fact, in our study we found several DET CYP genes belonging to flavonoid biosynthesis. Although few studies have investigated the specific response of flavonoid accumulation and expression in plants under waterlogging stress (Li et al., 2021; Wang et al., 2019), several genes encoding cytochrome P450 were responsive to waterlogging (Arbona et al., 2017; Li et al., 2021; Rastogi et al., 2020; Xu et al., 2017; Yin et al., 2017). The molecular and biochemical processes catalysed by CYPs have been extensively studied, particularly in model and crop plants (Pandian et al., 2020). Nevertheless, their effects on plant function, especially in non-model organisms, remain to be fully uncovered.

Several thioredoxins and glutaredoxins were differentially expressed between *Igapó* and *Terra firme* populations. They constitute families of thiol oxidoreductases belonging to key antioxidant systems providing defence against oxidative stress (Geigenberger et al., 2017; Hasanuzzaman et al., 2017; Meyer et al., 2012). These antioxidants interact with hormones and signalling molecules and act in detoxifying ROS, toxic metals and xenobiotics in plants facing salinity, drought, extreme temperature, heavy metals and light stress (Geigenberger et al., 2017; Hasanuzzaman et al., 2017).

Predictability and long-term duration of flooding in Amazonian rivers can enforce a pressure on individual performance strong enough to result in the evolutionary selection of conspicuous phenotypic differences between *terra firme* and floodplain populations as observed in *I. puberulus*. For instance, seedlings of the Central Amazonian tree *Himatanthus sucuuba* under flooding conditions show rapid formation of lenticels, adventitious roots and aerenchyma when facing submersion, and they also have greater concentrations of soluble sugars and starch in roots, larger seedling mass and accumulated more biomass in roots and stems in comparison to *Terra firme* seedlings (Ferreira et al., 2009). Investigations on the carbohydrate content of roots from some other Amazonian wetland tree species indicate that the demand for energy is met by translocating and storing carbohydrates in the roots during the terrestrial phase, which are then consumed during the flooding period (Scarano et al., 1994). Moreover, the oxygen released from adventitious roots in the oxygen-rich layer near the water surface also fosters the growth of harmful bacteria and fungi, prompting the activation of effective mechanisms against pathogens in the rhizosphere (De Simone et al., 2003).

In our study, we also identified DETs associated with light stresses. In *Igapó*, early light-induced protein 1 (ELIP) and chlorophyll(ide) b reductase NYC1 were overexpressed (Table S2). These genes are involved in response to high-light stress (Hutin et al., 2003; Sato et al., 2015). While ELIP photoprotective role involves chlorophyll binding during pigment-protein turnover or stabilizing assembly under light stress (Sato et al., 2015), NYC1 is the main enzyme responsible for the regulation of the level of chlorophyll b in *Arabidopsis*, maintaining the stability of photosystems under high-light conditions (Hutin et al., 2003). At this time we would like to emphasize that any stressful condition reducing the consumption of ATP and NADPH in photosynthesis (e.g. through limitation in CO_2 diffusion from atmosphere to chloroplasts or inhibition of RuBisCO activity) will cause an excessive energetic pressure in electron transport chain in thylakoids and then lead to oxidative stress. Therefore, those overexpressed genes linked initially to light stress are likely modulated by flooding, the most common stressor in *Igapó*. In fact, flooding is known to decrease photosynthesis in several Amazonian species (Parolin et al., 2001).

Interactions among gene expression profiles due to stress factors may enhance the tolerance and resilience to adverse environmental conditions (Mittler, 2006). Varied genomic approaches can offer new insights into biological phenomena of ecological and evolutionary significance. Studies of simultaneous abiotic stresses under controlled conditions are well documented in crop and model plants (Mittler, 2006), although molecular mechanisms underlying the abiotic responses of plants to a combination of stressors, which are common-place in the lifetime of a real organism in nature, are not well elucidated. These interactions are of great ecological relevance and may promote niche divergence and adaptations to extreme conditions (Roelofs et al., 2008). Altogether our

results demonstrate that differential gene expression determined by species' tolerance to flooding might also play a role in adaptive divergence among populations in the Amazonian riparian forests. While enrichment for pathways related to waterlogging stresses suggests they may facilitate acclimation to floodplain habitats, direct functional evidence validating their adaptive significance is still needed.

Specialization of tree species to Amazonian floodplains has been relatively well studied (Luize, Palma-Silva, et al., 2024; Parolin, 2009; Piedade et al., 2010). At the community level, the correlation between the phylogenetic composition of tree and forest types demonstrates that ecological selection impacts the distribution of Amazonian tree lineages (Luize, Bauman, et al., 2024); both *terra firme* and floodplain wetlands harbour many shared species in the Amazon region (Kubitzki, 1989; Luize, Bauman, et al., 2024). However, less understood are the processes operating at the microevolutionary scale within rapidly evolving lineages, as in ground herbs, which are often fully submerged during the peak of flooding. Additionally, the biogeographic processes and other evolutionary mechanisms involved in adapting to amphibious habitats remain understudied. Also important is the fact that flooding resulting from climate change is a real threat (Chevuturi et al., 2023) that will likely increase the risk of hypoxic stress, both in natural communities as in crop fields. The flood-adaptive genetic resources recovered here can inspire future conservation applications for riparian restoration.

Further studies that investigate the functional and ecological genomics of the candidate genes observed in this study will significantly enhance our understanding of their roles in local adaptation to environmental stresses encountered by *I. puberulus* in *Igapó* and *Terra firme* populations. For instance, conducting complementary common garden experiments and field transplantations to assess survival and fecundity across genotypes would provide essential functional gene validation. This approach will deepen our understanding of the non-exclusive role of local adaptation and plasticity in promoting population divergence in this important neotropical system. Additionally, mapping trait-associated loci would aid in establishing connections between phenotype and genotype. Furthermore, information about the pattern of growth (both below and above-ground) and also about physiological and biochemical responses of *I. puberulus* to flooding are essential to validate and confirm that the molecular responses related to gene expression were effective in improving plant performance in both sites. In such scenario, measurements of leaf gas exchange (photosynthesis/respiration and transpiration), primary photochemistry, leaf water status and sap flow, anaerobic and antioxidant metabolisms, hormonal balance, biomass production and partitioning and an in-depth characterization of the root system would prove the ecological performance proposed by gene expression.

AUTHOR CONTRIBUTIONS

Clarisse Palma-Silva designed the research, acquired the funding, conducted the fieldwork, collected the data and wrote the paper. Amanda F. Mortati conducted the fieldwork, collected the data and wrote the paper. Cleber Juliano Neves Chaves conducted the fieldwork, collected the data, and reviewed and edited versions of the manuscript. Bárbara Simões Santos Leal analysed the data and wrote the paper. Rafael V. Ribeiro reviewed and edited versions of the manuscript. Fabio Pinheiro reviewed and edited versions of the manuscript. Milene Ferro analysed the data, performed the research, and reviewed and edited versions of the manuscript. Diego M. Riaño-Pachón analysed the data, and reviewed and edited versions of the manuscript. Jacqueline Salvi de Mattos analysed the data, and reviewed and edited versions of the manuscript. Marília Manupella Tavares analysed the data, and reviewed and edited versions of the manuscript. Paulo Aecyo analysed the data, and reviewed and edited versions of the manuscript. Tami da Costa Cacossi collected the data, reviewed and edited versions of the manuscript. Jochen Schöngart acquired funding, performed research, and reviewed and edited versions of the manuscript. Maria Teresa Fernandez Piedade acquired funding, and reviewed and edited versions of the manuscript. Thiago André designed the research, acquired funding, conducted fieldwork, collected the data and wrote the paper. All authors helped improve the final version of the manuscript.

ACKNOWLEDGEMENTS

This work has been supported by the following Brazilian research agencies: São Paulo Research Foundation (FAPESP Grants: 2019/24823-2, 2021/10639-5), Fundação Amazônia de Amparo a Estudos e Pesquisas (FAPESPA), Coordenação de Aperfeiçoamento de Pessoal de Nível Superior—Brasil (CAPES)—Código de Financiamento 001, and the National Council for Scientific and Technological Development (CNPq, Brazil). C.P-S. is a fellow of CNPq (302962/2022-0). T.A. was funded by the grant 067/2020 (FAPESPA). D.M.R.P. is a fellow of CNPq (311558/2021-6). R.V.R. is a fellow of CNPq (Grant 304295/2022-1). F.P. is a fellow of CNPq (302849/2021-1). The authors are also thankful to Chico Mendes Institute for Biodiversity Conservation ("ICMBIO", Portuguese acronym) collection permits and to the FLONA Tapajós community "São Francisco do Godinho" for logistic support during field work. We thank Leidiane Oliveira for all support with environmental data sampling.

CONFLICT OF INTEREST STATEMENT

The authors declare no conflict of interest.

DATA AVAILABILITY STATEMENT

The diploid genome shotgun assembly project has been deposited at the DDBJ/EMBL/GenBank, haplophase 1 under the Bioproject PRJNA1095439 and haplophase 2 under the Bioproject PRJNA1095438. This Transcriptome Shotgun Assembly project has been deposited at DDBJ/EMBL/GenBank under the accession GKTN00000000. The version described in this paper is the first version, GKTN01000000. Sequencing reads have been deposited at the Short Read Archive (SRA) under the following accessions: PacBio HiFi SRR28549781; OmniC SRR28549780; RNA-Seq SRR28549739 to SRR28549779. All the above data submitted at NCBI databases

can be accessed under the umbrella BioProject PRJNA1099595. Genomic variants, transcriptome functional annotation and genome annotation (gene prediction) are available from Figshare under https://doi.org/10.6084/m9.figshare.25607139.

ORCID

Clarisse Palma-Silva https://orcid.org/0000-0003-0192-5489
Cleber Juliano Neves Chaves https://orcid.org/0000-0002-5960-7304
Bárbara Simões Santos Leal https://orcid.org/0000-0003-4401-3252
Fabio Pinheiro https://orcid.org/0000-0003-3243-2652

REFERENCES

Alexa, A., & Rahnenfuhrer, J. (2010). *topGO: Enrichment analysis for gene ontology*. R package version, 2(0), 2010.

Andersson, L. (1977). The genus *Ischnosiphon* (Marantaceae). *Opera Botanica*, *43*, 1–113.

Arbona, V., Zandalinas, S. I., Manzi, M., González-Guzmán, M., Rodriguez, P. L., & Gómez-Cadenas, A. (2017). Depletion of abscisic acid levels in roots of flooded Carrizo citrange (*Poncirus trifoliata* L. Raf. × *Citrus sinensis* L. Osb.) plants is a stress-specific response associated to the differential expression of PYR/PYL/RCAR receptors. *Plant Molecular Biology*, *93*, 623–640.

Ashraf, M. A. (2012). Waterlogging stress in plants: A review. *African Journal of Agricultural Research*, *7*(13), 1976–1981.

Bleich, M. E., Mortati, A. F., André, T., & Piedade, M. T. F. (2014). Riparian deforestation affects the structural dynamics of headwater streams in Southern Brazilian Amazonia. *Tropical Conservation Science*, *7*(4), 657–676.

Blokhina, O., Virolainen, E., & Fagerstedt, K. V. (2003). Antioxidants, oxidative damage and oxygen deprivation stress: A review. *Annals of Botany*, *91*(2), 179–194.

Brousseau, L., Fine, P. V., Dreyer, E., Vendramin, G. G., & Scotti, I. (2021). Genomic and phenotypic divergence unveil microgeographic adaptation in the Amazonian hyperdominant tree Eperua falcata Aubl. (Fabaceae). *Molecular Ecology*, *30*(5), 1136–1154.

Brůna, T., Hoff, K. J., Lomsadze, A., Stanke, M., & Borodovsky, M. (2021). BRAKER2: Automatic eukaryotic genome annotation with GeneMark-EP+ and AUGUSTUS supported by a protein database. *NAR Genomics and Bioinformatics*, *3*(1), lqaa108. https://doi.org/10.1093/nargab/lqaa108

Bushnell, B. (2014). BBMap: a fast, accurate, splice-aware aligner.

Cheng, H., Concepcion, G. T., Feng, X., Zhang, H., & Li, H. (2021). Haplotype-resolved de novo assembly using phased assembly graphs with hifiasm. *Nature Methods*, *18*(2), 170–175.

Chevuturi, A., Klingaman, N. P., Woolnough, S. J., Rudorff, C. M., Coelho, C. A. S., & Schöngart, J. (2023). Forecasting annual maximum water level for the Negro River at Manaus using dynamical seasonal predictions. *Climate Services*, *30*, 100342. https://doi.org/10.1016/j.cliser.2023.100342

Costa, F. R. C. (2004). Structure and composition of the ground-herb community in a terra-firme Central Amazonian forest. *Acta Amazônica*, *34*(1), 53–59.

Danecek, P., Auton, A., Abecasis, G., Albers, C. A., Banks, E., DePristo, M. A., Handsaker, R. E., Lunter, G., Marth, G. T., Sherry, S. T., McVean, G., Durbin, R., & 1000 Genomes Project Analysis Group. (2011). The variant call format and VCFtools. *Bioinformatics*, *27*(15), 2156–2158.

Danecek, P., Bonfield, J. K., Liddle, J., Marshall, J., Ohan, V., Pollard, M. O., Whitwham, A., Keane, T., McCarthy, S. A., Davies, R. M., & Li, H. (2021). Twelve years of SAMtools and BCFtools. *GigaScience*, *10*(2), giab008.

De Simone, O., Haase, K., Müller, E., Junk, W., Hartmann, K., Schreiber, L., & Schmidt, W. (2003). Apoplasmic barriers and oxygen transport properties of Hypoder- mal cell walls in roots from four Amazonian tree species. *Plant Physiology*, *132*, 206–217.

DePristo, M. A., Banks, E., Poplin, R., Garimella, K. V., Maguire, J. R., Hartl, C., Philippakis, A. A., del Angel, G., Rivas, M. A., Hanna, M., McKenna, A., Fennell, T. J., Kernytsky, A. M., Sivachenko, A. Y., Cibulskis, K., Gabriel, S. B., Altshuler, D., & Daly, M. J. (2011). A framework for variation discovery and genotyping using next-generation DNA sequencing data. *Nature Genetics*, *43*(5), 491–498.

Dobin, A., & Gingeras, T. R. (2015). Mapping RNA-seq reads with STAR. *Current Protocols in Bioinformatics*, *51*(1), 11–14.

Doyle, J. J., & Doyle, J. L. (1987). A rapid DNA isolation procedure for small quantities of fresh leaf tissue. *Phytochemical Bulletin*, *19*, 11–15.

Drucker, D., Costa, F., & Magnusson, W. (2008). How wide is the riparian zone of small streams in tropical forests? A test with terrestrial herbs. *Journal of Tropical Ecology*, *24*(1), 65–74.

Duivenvoorden, J. F., & Lips, J. M. (1995). *A land-ecological study of soils, vegetation, and plant diversity in Colombian Amazonia. Tropenbos series 12*. Tropenbos.

Earl, D. A., & VonHoldt, B. M. (2012). STRUCTURE HARVESTER: A website and program for visualizing STRUCTURE output and implementing the Evanno method. *Conservation Genetics Resources*, *4*, 359–361.

Falush, D., Stephens, M., & Pritchard, J. K. (2003). Inference of population structure using multilocus genotype data: Linked loci and correlated allele frequencies. *Genetics*, *164*(4), 1567–1587.

Ferreira, C. S., Piedade, M. T. F., Franco, A. C., Gonçalves, J. F. C., & Junk, W. J. (2009). Adaptive strategies to tolerate prolonged flooding in seedlings of floodplain and upland populations of *Himatanthus sucuuba*, a Central Amazon tree. *Aquatic Botany*, *90*(3), 246–252.

Flynn, J. M., Hubley, R., Goubert, C., Rosen, J., Clark, A. G., Feschotte, C., & Smit, A. F. (2020). RepeatModeler2 for automated genomic discovery of transposable element families. *Proceedings of the National Academy of Sciences of the United States of America*, *117*(17), 9451–9457. https://doi.org/10.1073/pnas.1921046117

Geigenberger, P., Thormählen, I., Daloso, D. M., & Fernie, A. R. (2017). The unprecedented versatility of the plant thioredoxin system. *Trends in Plant Science*, *22*(3), 249–262.

Gentry, A. H., & Emmons, L. H. (1987). Geographical variation in fertility, phenology, and composition of the understory of Neotropical forests. *Biotropica*, *19*(3), 216–227.

Götz, S., García-Gómez, J. M., Terol, J., Williams, T. D., Nagaraj, S. H., Nueda, M. J., Robles, M., Talón, M., Dopazo, J., & Conesa, A. (2008). High-throughput functional annotation and data mining with the Blast2GO suite. *Nucleic Acids Research*, *36*(10), 3420–3435.

Goudet, J. (2005). Hierfstat, a package for R to compute and test hierarchical F-statistics. *Molecular Ecology Notes*, *5*(1), 184–186.

Grabherr, M. G., Haas, B. J., Yassour, M., Levin, J. Z., Thompson, D. A., Amit, I., Adiconis, X., Fan, L., Raychowdhury, R., Zeng, Q., Chen, Z., Mauceli, E., Hacohen, N., Gnirke, A., Rhind, N., di Palma, F., Birren, B. W., Nusbaum, C., Lindblad-Toh, K., … Regev, A. (2011). Trinity: Reconstructing a full-length transcriptome without a genome from RNA-Seq data. *Nature Biotechnology*, *29*(7), 644–652.

Gregory, S. V., Swanson, F. J., Mckee, W. A., & Cummins, K. W. (1991). An ecosystem perspective of riparian zones: Focus on links between land and water. *Bioscience*, *41*(8), 540–551.

Gu, Z., Gu, L., Eils, R., Schlesner, M., & Brors, B. (2014). Circlizeimplements and enhances circular visualization in R. *Bioinformatics*, *30*(19), 2811–2812.

Gupta, D. K., Palma, J. M., & Corpas, F. J. (2016). *Redox state as a central regulator of plant-cell stress response*. Springer.

Gurevich, A., Saveliev, V., Vyahhi, N., & Tesler, G. (2013). QUAST: Quality assessment tool for genome assemblies. *Bioinformatics*, *29*(8), 1072–1075.

Haas, B. J., Papanicolaou, A., Yassour, M., Grabherr, M., Blood, P. D., Bowden, J., Couger, M. B., Eccles, D., Li, B., Lieber, M. D., MacManes,

M. M., Ott, M., Orvis, J., Pochet, N., Strozzi, F., Weeks, N., Westerman, R., William, T., Dewey, C. N., … Regev, A. (2013). De novo transcript sequence reconstruction from RNA-seq using the Trinity platform for reference generation and analysis. *Nature Protocols*, *8*(8), 1494–1512.

Hansen, C. C., Nelson, D. R., Møller, B. L., & Werck-Reichhart, D. (2021). Plant cytochrome P450 plasticity and evolution. *Molecular Plant*, *14*(8), 1244–1265.

Hasanuzzaman, M., Nahar, K., Anee, T. I., & Fujita, M. (2017). Glutathione in plants: biosynthesis and physiological role in environmental stress tolerance. *Physiology and Molecular Biology of Plants*, *23*, 249–268.

Herrera, R., Jordan, C. F., Klinge, H., & Medina, E. (1978). Amazon ecosystems—Their structure and functioning with particular emphasis on nutrients. *Interciencia*, *3*(4), 223–232.

Howe, K., Chow, W., Collins, J., Pelan, S., Pointon, D.- L., Sims, Y., Torrance, J., Tracey, A., & Wood, J. (2021). Significantly improving the quality of genome assemblies through curation. *GigaScience*, *10*(1), giaa153. https://doi.org/10.1093/gigascience/giaa153

Hutin, C., Nussaume, L., Moise, N., Moya, I., Kloppstech, K., & Havaux, M. (2003). Early light-induced proteins protect Arabidopsis from photooxidative stress. *Proceedings of the National Academy of Sciences of the United States of America*, *100*(8), 4921–4926.

Junk, W. J. (1989). Flood tolerance and tree distribution in central Amazonian floodplains. In L. B. Holm-Nielsen, I. C. Nielsen, & H. Balslev (Eds.), *Tropical forests: Botanical dynamics, speciation and diversity* (pp. 47–64). Academic Press.

Junk, W. J., & Piedade, M. T. F. (1997). Plant life in the floodplain with special reference to herbaceous plants. In W. J. Junk (Ed.), *Ecological studies, Vol. 126. The Central Amazon floodplain* (pp. 147–185). Springer-Verlag.

Junk, W. J., Piedade, M. T. F., Schöngart, J., Cohn-Haft, M., Adeney, J. M., & Wittmann, F. (2011). A classification of major naturally-occurring Amazonian lowland wetlands. *Wetlands*, *31*, 623–640.

Keenan, K., McGinnity, P., Cross, T. F., Crozier, W. W., & Prodöhl, P. A. (2013). diveRsity: An R package for the estimation and exploration of population genetics parameters and their associated errors. *Methods in Ecology and Evolution*, *4*(8), 782–788.

Kopelman, N. M., Mayzel, J., Jakobsson, M., Rosenberg, N. A., & Mayrose, I. (2015). Clumpak: A program for identifying clustering modes and packaging population structure inferences across K. *Molecular Ecology Resources*, *15*(5), 1179–1191.

Kubitzki, K. (1989). The ecogeographical differentiation of Amazonian inundation forests. *Plant Systematics and Evolution*, *162*, 285–304.

Laetsch, D. R., & Blaxter, M. L. (2017). BlobTools: Interrogation of genome assemblies. *F1000Research*, *6*, 1287. https://doi.org/10.12688/f1000research.12232.1

Leal, B. S. S., Brandão, M. M., Palma-Silva, C., & Pinheiro, F. (2020). Differential gene expression reveals mechanisms related to habitat divergence between hybridizing orchids from the Neotropical coastal plains. *BMC Plant Biology*, *20*, 1–14.

Li, B., & Dewey, C. N. (2011). RSEM: Accurate transcript quantification from RNA-Seq data with or without a reference genome. *BMC Bioinformatics*, *12*, 1–16.

Li, Y., Shi, L. C., Yang, J., Qian, Z. H., He, Y. X., & Li, M. W. (2021). Physiological and transcriptional changes provide insights into the effect of root waterlogging on the aboveground part of *Pterocarya stenoptera*. *Genomics*, *113*, 2583–2590.

López-Maury, L., Marguerat, S., & Bähler, J. (2008). Tuning gene expression to changing environments: From rapid responses to evolutionary adaptation. *Nature Reviews. Genetics*, *9*, 583–593.

Luize, B. G., Bauman, D., ter Steege, H., Palma-Silva, C., do Amaral, I. L., de Souza Coelho, L., de Almeida Matos, F. D., de Andrade Lima Filho, D., Salomão, R. P., Wittmann, F., Castilho, C. V., de Jesus Veiga Carim, M., Guevara, J. E., Phillips, O. L., Magnusson, W. E., Sabatier, D., Revilla, J. D. C., Molino, J.-F., Irume, M. V., … Dexter, K. G. (2024). Geography and ecology shape the phylogenetic composition of Amazonian tree communities. *Journal of Biogeography*, *51*, 1163–1184. https://doi.org/10.1111/jbi.14816

Luize, B. G., Palma-Silva, C., Siqueira, T., & Silva, T. S. F. (2024). Tree species occurring in Amazonian wetland forests consistently show broader range sizes and niche breadths than trees in upland forests. *Ecology and Evolution*, *14*, e11230.

Luo, W., Zhao, Z., Chen, H., Ao, W., Lu, L., Liu, J., Li, X., & Sun, Y. (2023). Genome-wide characterization and expression of DELLA genes in *Cucurbita moschata* reveal their potential roles under development and abiotic stress. *Frontiers in Plant Science*, *14*, 1137126.

Manni, M., Berkeley, M. R., Seppey, M., & Zdobnov, E. M. (2021). BUSCO: Assessing genomic data quality and beyond. *Current Protocols*, *1*(12), e323.

Meyer, Y., Belin, C., Delorme-Hinoux, V., Reichheld, J. P., & Riondet, C. (2012). Thioredoxin and glutaredoxin systems in plants: Molecular mechanisms, crosstalks, and functional significance. *Antioxidants & Redox Signaling*, *17*(8), 1124–1160.

Mittler, R. (2006). Abiotic stress, the field environment and stress combination. *Trends in Plant Science*, *11*(1), 15–19.

Nosil, P. (2012). *Ecological speciation*. Oxford University Press.

Oksanen, J., Simpson, G., Blanchet, F. G., Kindt, R., Legendre, P., Minchin, P. R., O'Hara, R. B., Solymos, R., Stevens, M. H., Szoecs, E., Wagner, H., Barbour, M., Bedward, M., Bolker, B., Borcard, D., Carvalho, G., Chirico, M., Caceres, M., Durand, S., … Weedon, J. (2022). Vegan: Community ecology package, Version 2.6-4.

Pandian, B. A., Sathishraj, R., Djanaguiraman, M., Prasad, P. V., & Jugulam, M. (2020). Role of cytochrome P450 enzymes in plant stress response. *Antioxidants*, *9*(5), 454.

Paquette, S. R., & Paquette, M. S. R. (2011). *Package 'PopGenKit'*.

Parolin, P. (2009). Submerged in darkness: Adaptations to prolonged submergence by woody species of the Amazonian floodplains. *Annals of Botany*, *103*, 359–376.

Parolin, P., De Simone, O., Haase, K., Waldhoff, D., Rottenberger, S., Kuhn, U., Kesselmeier, J., Kleiss, B., Schmidt, W., Piedade, M. T. F., & Junk, W. J. (2004). Central Amazonian floodplain forests: Tree adaptations in a pulsing system. *The Botanical Review*, *70*, 357–380.

Parolin, P., Junk, W. J., & Piedade, M. T. F. (2001). Gas exchange of six tree species from Central Amazonian floodplains. *Tropical Ecology*, *42*(1), 15–24.

Penna, S., & Naithani, S. (2022). Understanding the plant's response to global climate change using Omics. *Current Plant Biology*, *29*, 100241.

Piedade, M. T. F., Ferreira, C. S., Wittmann, A. D. O., Buckeridge, M., & Parolin, P. (2010). Biochemistry of Amazonian floodplain trees. In W. Junk, M. Piedade, F. Wittmann, J. Schöngart, & P. Parolin (Eds.), *Amazonian floodplain forests. Ecological studies* (Vol. *210*). Springer.

Poulsen, A. D., & Balslev, H. (1991). Abundance and cover of ground herbs in an Amazonian rain forest. *Journal of Vegetation Science*, *2*, 315–322.

Pritchard, J. K., Stephens, M., & Donnelly, P. (2000). Inference of population structure using multilocus genotype data. *Genetics*, *155*(2), 945–959.

Quast, C., Pruesse, E., Yilmaz, P., Gerken, J., Schweer, T., Yarza, P., Peplies, J., & Glöckner, F. O. (2012). The SILVA ribosomal RNA gene database project: Improved data processing and web-based tools. *Nucleic Acids Research*, *41*(D1), D590–D596.

Raffini, F., Schneider, R. F., Franchini, P., Kautt, A. F., & Meyer, A. (2020). Diving into divergence: Differentiation in swimming performances, physiology and gene expression between locally-adapted sympatric cichlid fishes. *Molecular Ecology*, *29*(7), 1219–1234.

Rastogi, S., Satapathy, S., Shah, S., & Prakash, H. G. (2020). In silico identification of cytochrome P450s involved in *Ocimum tenuiflorum* subjected to four abiotic stresses. *Gene Reports*, *20*, 100781.

Renault, H., Bassard, J. E., Hamberger, B., & Werck-Reichhart, D. (2014). Cytochrome P450-mediated metabolic engineering: Current progress and future challenges. *Current Opinion in Plant Biology*, *19*, 27–34.

Rhie, A., Walenz, B. P., Koren, S., & Phillippy, A. M. (2020). Merqury: Reference-free quality, completeness, and phasing assessment for genome assemblies. *Genome Biology*, *21*, 245.

Rivera, H. E., Aichelman, H. E., Fifer, J. E., Kriefall, N. G., Wuitchik, D. M., Smith, S. J., & Davies, S. W. (2021). A framework for understanding gene expression plasticity and its influence on stress tolerance. *Molecular Ecology*, *30*(6), 1381–1397.

Robinson, M. D., McCarthy, D. J., & Smyth, G. K. (2010). edgeR: A Bioconductor package for differential expression analysis of digital gene expression data. *Bioinformatics*, *26*(1), 139–140.

Roelofs, D., Aarts, M. G. M., Schat, H., & Van Straalen, N. M. (2008). Functional ecological genomics to demonstrate general and specific responses to abiotic stress. *Functional Ecology*, *22*(1), 8–18.

Santana, F. D., Baccaro, F. B., & Costa, F. R. C. (2016). Busy nights: High seed dispersal by crickets in a Neotropical Forest. *American Naturalist*, *188*(5), E126–E133.

Santos, B. N. V., Silva, J. C., & Clarindo, W. R. (2022). The landscape of karyotype diversity in Marantaceae. *Scientia Horticulturae*, *299*, 111044.

Sato, R., Ito, H., & Tanaka, A. (2015). Chlorophyll *b* degradation by chlorophyll *b* reductase under high-light conditions. *Photosynthesis Research*, *126*, 249–259.

Scarano, F. R., Cattânio, J. H., & Crawford, R. M. M. (1994). Root carbohydrates storage in young saplings of an Amazonian tidal Várzea Forest before the onset of the wet season. *Acta Botanica Brasilicia*, *8*, 129–139.

Schietti, J., Emilio, T., Rennó, C. D., Drucker, D. P., Costa, F. R. C., Nogueira, A., Baccaro, F. B., Figueiredo, F., Castilho, C. V., Kinupp, V., Guillaumet, J. L., Garcia, A. R. M., Lima, A. P., & Magnusson, W. E. (2014). Vertical distance from drainage drives floristic composition changes in an Amazonian rainforest. *Plant Ecology & Diversity*, *7*(1–2), 241–253.

Schluter, D. (2009). Evidence for ecological speciation and its alternative. *Science*, *323*(5915), 737–741.

Shomali, A., Das, S., Arif, N., Sarraf, M., Zahra, N., Yadav, V., Aliniaeifard, S., & Hasanuzzaman, M. (2022). Diverse physiological roles of flavonoids in plant environmental stress responses and tolerance. *Plants*, *11*(22), 3158.

Simão, F. A., Waterhouse, R. M., Ioannidis, P., Kriventseva, E. V., & Zdobnov, E. M. (2015). BUSCO: Assessing genome assembly and annotation completeness with single-copy orthologs. *Bioinformatics*, *31*(19), 3210–3212.

Soares, E. S. (2004). *A Floresta Nacional do Tapajós: desafios, resultados, ameaças e oportunidades em uma unidade de conservação na Amazônia*. IBAMA/PROMANEJO.

Song, L., & Florea, L. (2015). Rcorrector: Efficient and accurate error correction for Illumina RNA-seq reads. *GigaScience*, *4*(1), S13742-015.

Spicer, M. E., Mellor, H., & Carson, W. P. (2020). Seeing beyond the trees: A comparison of tropical and temperate plant growth-forms and their vertical distribution. *Ecology*, *101*(4), e02974.

Supek, F., Bošnjak, M., Škunca, N., & Šmuc, T. (2011). REVIGO summarizes and visualizes long lists of gene ontology terms. *PLoS One*, *6*(7), e21800.

Tarailo-Graovac, M., & Chen, N. (2009). Using RepeatMasker to identify repetitive elements in genomic sequences. *Current Protocols in Bioinformatics*, *Chapter 4*, 4.10.1–4.10.14.

Ungerer, M., Johnson, L., & Herman, M. (2008). Ecological genomics: Understanding gene and genome function in the natural environment. *Heredity*, *100*, 178–183.

Van der Auwera, G. A., Carneiro, M. O., Hartl, C., Poplin, R., Del Angel, G., Levy-Moonshine, A., Jordan, T., Shakir, K., Roazen, D., Thibault, J., Banks, E., Garimella, K. V., Altshuler, D., Gabriel, S., & DePristo, M. A. (2013). From FastQ data to high-confidence variant calls: The genome analysis toolkit best practices pipeline. *Current Protocols in Bioinformatics*, *43*(1), 10–11.

Van Straalen, N. M., & Roelofs, D. (2011). *An introduction to ecological genomics*. OUP Oxford.

Veloso, H. P., Rangel Filho, A. L. R., & Lima, J. C. A. (1991). *Classificação da vegetação brasileira, adaptada a um sistema universal* (123 p.). IBGE.

Vurture, G. W., Sedlazeck, F. J., Nattestad, M., Underwood, C. J., Fang, H., Gurtowski, J., & Schatz, M. C. (2017). GenomeScope: Fast reference-free genome profiling from short reads. *Bioinformatics*, *33*(14), 2202–2204.

Wang, T., Zou, Q., Guo, Q., Yang, F., Wu, L., & Zhang, W. (2019). Widely targeted metabolomics analysis reveals the effect of flooding stress on the synthesis of flavonoids in *Chrysanthemum morifolium*. *Molecules*, *24*, 3695.

Wittmann, F., Schongart, J., Brito, J. M., Wittmann, A. O., Piedade, M. T. F., Parolin, P., Junk, W. J., & Guillaumet, J. L. (2010). *Manual of trees from central Amazonian Várzea floodplains: Taxonomy, ecology and use*. INPA.

Xu, X., Chen, M., Ji, J., Xu, Q., Qi, X., & Chen, X. (2017). Comparative RNA-seq based transcriptome profiling of waterlogging response in cucumber hypocotyls reveals novel insights into the de novo adventitious root primordia initiation. *BMC Plant Biology*, *17*(129), 1–13.

Yin, X., Hiraga, S., Hajika, M., Nishimura, M., & Komatsu, S. (2017). Transcriptomic analysis reveals the flooding tolerant mechanism in flooding tolerant line and abscisic acid treated soybean. *Plant Molecular Biology*, *93*, 479–496.

Zdobnov, E. M., & Apweiler, R. (2001). InterProScan–an integration platform for the signature-recognition methods in InterPro. *Bioinformatics*, *17*(9), 847–848.

Zhou, C., McCarthy, S. A., & Durbin, R. (2023). YaHS: yet another Hi-C scaffolding tool. *Bioinformatics*, *39*(1), btac808.

SUPPORTING INFORMATION

Additional supporting information can be found online in the Supporting Information section at the end of this article.

How to cite this article: Palma-Silva, C., Mortati, A. F., Chaves, C. J. N., Simões Santos Leal, B., Ribeiro, R. V., Pinheiro, F., Ferro, M., Riaño-Pachón, D. M., de Mattos, J. S., Tavares, M. M., Aecyo, P., da Costa Cacossi, T., Schöngart, J., Piedade, M. T. F., & André, T. (2024). Ecological transcriptomics reveals stress response pathways of a ground-herb species in a waterlogging gradient of Amazonian riparian forests. *Molecular Ecology*, *00*, e17437. https://doi.org/10.1111/mec.17437